
Title	Remote plasma-assisted low-temperature large-area graphene synthesis
Author(s)	Jian Yi Pae, Rohit Medwal, Joseph Vimal Vas, Murukeshan Vadakke Matham, and Rajdeep Singh Rawat
Source	<i>Journal of Vacuum Science & Technology B</i> , 37: 041201
Published by	AIP Publishing

Copyright © 2019 The Authors

This document may be used for private study or research purpose only. This document or any part of it may not be duplicated and/or distributed without permission of the copyright owner.

The Singapore Copyright Act applies to the use of this document.

Citation: Pae, J. Y., Rohit Medwal, Joseph Vimal Vas, Murukeshan Vadakke Matham, & Rawat, S. R. (2019). Remote plasma-assisted low-temperature large-area graphene synthesis. *Journal of Vacuum Science & Technology B*, 37: 041201. <http://dx.doi.org/10.1116/1.5093241>

This document was archived with permission from the copyright holder.



Remote plasma-assisted low-temperature large-area graphene synthesis

Jian Yi Pae,^{1,2} Rohit Medwal,³ Joseph Vimal Vas,³ Murukeshan Vadakke Matham,^{1,2,a)} and Rajdeep Singh Rawat^{3,b)}

¹Singapore Centre for 3D Printing, School of Mechanical and Aerospace Engineering, Nanyang Technological University, Singapore 639798

²Centre for Optical and Laser Engineering (COLE), Nanyang Technological University, Singapore 639798

³Natural Sciences and Science Education, National Institute of Education, Nanyang Technological University, Singapore 637616

(Received 19 February 2019; accepted 13 May 2019; published 29 May 2019)

Graphene is typically grown using thermal chemical vapor deposition (CVD) on metallic substrates such as copper and nickel at elevated temperatures above 1000 °C. The synthesis of large-area graphene at low temperature is highly desirable for large volume industrial production. In this paper, the authors report a remote plasma-assisted CVD graphene synthesis at a reduced temperature of 600 °C in a relatively shorter duration of 15 min. Scanning electron microscopy reveals the formation of large graphene crystal with an approximate size of $100 \times 100 \mu\text{m}^2$ over the entire $2 \times 10 \text{ cm}^2$ surface of copper foil substrates. Raman spectra recorded for graphene grown at 600 °C show the presence of a graphene characteristic “2D” peak, attesting to the formation of graphene. The results show that it is possible to grow horizontal graphene at low temperatures and transfer it to flexible polyethylene terephthalate substrates. The utility of the synthesized graphene is ascertained through the successful fabrication of a flexible graphene-based electrochemical sensor for the detection of glucose concentration. The present research will have a direct impact on flexible wearable biosensors. *Published by the AVS.* <https://doi.org/10.1116/1.5093241>

I. INTRODUCTION

One of the most significant discoveries of the 21st century is the successful isolation of one-atomic layer thick 2D carbon (graphene) from graphite.¹ Due to its unique 2D structure, graphene demonstrates high charge carrier mobility at room temperature that exceeds $2.0 \times 10^5 \text{ cm}^2 \text{ V}^{-1} \text{ s}^{-1}$ (more than 100 times that of silicon)² with high thermal conductivity of about 5000 W/mK. Besides that, graphene is also about 98% optically transparent in the visible wavelength band,³ which makes it ideal for optical devices. In addition, graphene acts as an excellent substrate for the immobilization of biomolecules which could improve the long-term stability of biosensors.⁴ Therefore, coupled with its wonderlike properties, graphene is a highly attractive material for the development of biosensors with enhanced sensitivity and selectivity.

The method for growing graphene has improved significantly over the years.⁵ The very first sample of graphene was isolated from graphite using a mechanical exfoliation method which used a scotch tape to repeatedly stick and pull apart the graphite layers.⁶ This method is novel but slow and could only yield small flakes of graphene of random layers which may have either very limited or no practical uses. Nonetheless, it demonstrated the possibility of creating 2D graphene and allowed researchers to report on its excellent electrical properties. Since then, many modern methods such as mechanical cleaving, chemical exfoliation, chemical synthesis, and thermal chemical vapor deposition (CVD) have been widely reported for the synthesis of graphene.^{7,8}

Among these, CVD is the conventional method for large-scale synthesis of high-quality graphene.⁹

The major challenge of using a pure CVD process for graphene synthesis is that it requires very high temperature (>1000 °C) to catalyze the reaction and a significantly long synthesis duration.^{10,11} Alternatively, by utilizing plasma enhanced CVD (PECVD), the growth of the graphene has been realized at a lower processing temperature of around 700 °C with a relatively reduced growth duration.^{12–14} The use of nonthermal plasma (with electron temperature much higher than ion/gas temperature) facilitates the efficient production of carbon radicals through the electron impact dissociation of carbon precursor feed resulting in graphene synthesis at a lower temperature.¹⁵ The conventional PECVD method involves the placement of substrates within the plasma volume which mostly results in the growth of vertical graphene¹⁶ on the substrates due to a high electric field caused by plasma sheath formation.

In this paper, we report the use of a remote-plasma CVD as a method for large-area horizontal graphene synthesis, wherein the heated reaction chamber is separated and placed downstream from the plasma generation region. We demonstrate the remote plasma-based synthesis of large-area graphene at a reduced temperature as low as 600 °C and successful use of this graphene for electrochemical glucose sensor.

II. EXPERIMENTAL SETUP AND METHODOLOGY

A. Graphene synthesis at low temperature

The schematic diagram of the integrated remote-plasma CVD setup is shown in Fig. 1. It may be noted that the feed gas first passes through the capacitively coupled radio

^{a)}Electronic mail: mmurukeshan@ntu.edu.sg

^{b)}Electronic mail: rajdeep.rawat@nie.edu.sg

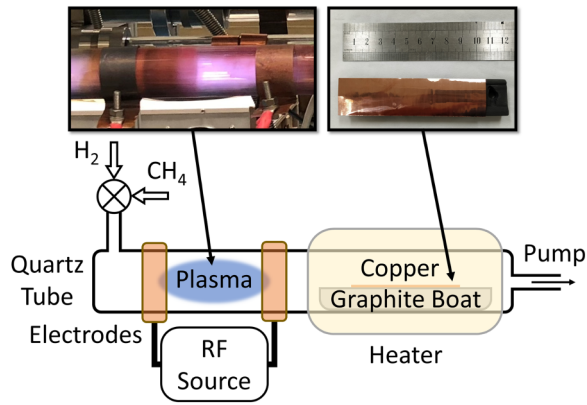


FIG. 1. Schematic diagram of the remote plasma-assisted CVD setup.

frequency (RF) plasma region before proceeding into the well-separated heated CVD reaction chamber placed downstream. Prior to growth, copper (Cu) foil (MTI Corporation), with a thickness of approximately $25\ \mu\text{m}$, is trimmed to $10 \times 2\ \text{cm}^2$ large pieces to be used as the growth substrate. The Cu substrates are then cleaned with acetone (in sonication bath) and washed with de-ionized (DI) water, followed by a second cleaning with isopropyl alcohol (in sonication bath) and DI water wash to thoroughly remove any native oxide or surface contaminants. The cleaned substrate is then placed within a 40 mm diameter horizontal quartz tube which serves as the CVD reaction chamber and a 30 cm long ceramic heater is positioned with the copper substrate at its center to ensure uniform heating across the substrate. Next, the quartz tube is sealed and evacuated to the base pressure of below 10^{-2} mbar, after which hydrogen (H_2) gas is introduced at a flow rate of 2 standard cubic centimeters per minute (sccm). In order to improve the quality of the deposited material, the surface of the Cu foil is etched¹⁷ by raising to a reactor chamber temperature to about $1040\ ^\circ\text{C}$ for 15 min. Thereafter, the temperature of the reaction chamber is reduced to and controlled at 1000, 800, 600, and $400\ ^\circ\text{C}$, respectively, to investigate the lowest deposition temperature. Once the desired reactor chamber temperature is achieved, methane (CH_4) gas is introduced at 10 sccm flow rate into the reaction chamber and at the same time, the capacitively coupled remote plasma is switched on using a 13.56 MHz RF power supply at 100 W. After 15 min, the methane supply and the RF power supply are turned off and the reaction chamber is rapidly cooled down to room temperature under the flow of H_2 .

B. Optical emission spectroscopy

The plasma parameters such as the electron temperature have a significant influence on the quality of the graphene synthesized using PECVD. Since the plasma parameters are governed by the physical parameters, it is necessary to quantify these parameters (for example, the dimensions of the quartz tube, electrode space, gas used, RF power, etc.) to ensure the repeatability of the experiment. Optical emission spectroscopy (OES) is preferred in this study since the

measurements are noninvasive and can provide an estimation of the plasma temperature by examining the wavelengths of photons emitted by atoms or molecules during their transition from an excited state to a lower energy state.¹⁸ The OES was done using a spectrometer (Ocean Optics, USB 4000 vis-NIR), and the spectrum of a CH_4/H_2 plasma at an RF power of 100 W is shown in Fig. 2. The plasma temperature is then calculated from the spectra using the line ratio method, assuming that the plasma is in local thermal equilibrium and that the spectra are optically thin.¹⁹ The intensity of the spectral line is given by²⁰

$$I_{ij} = \frac{hcA_{ij}g_jn}{\lambda_{ij}U(T)} e^{(E_j/kT)}, \quad (1)$$

where I_{ij} and λ_{ij} are the intensity and wavelength corresponding to transition from i to j , respectively, h is Planck's constant, c is the speed of light, n is the number density of emitting species, $U(T)$ is the partition function, A_{ij} is the transition probability between level i and j , k is Boltzmann's constant, T is the excitation temperature, g_j is the statistical weight of upper energy level, and E_j is the upper energy level in eV unit.

Taking the intensity ratio of two spectral lines of the same species and ionization stage, the line ratio can be expressed as

$$\frac{I_1}{I_2} = \frac{g_1 A_1 \lambda_2}{g_2 A_2 \lambda_1} e^{[-(E_1 - E_2)/kT]}, \quad (2)$$

where I is the intensity, g is the statistical weight, A is the transition probability, λ is the wavelength, E is the energy of excited state in eV, and k is Boltzmann constant.

The electron temperature of the hydrogen plasma can then be estimated from the corresponding H_α and H_β spectral lines as shown in Fig. 2. The plasma temperature at 100 W RF power was found to be 1.38 eV, and distinct lines were found in the 386–390 and 430–435 nm range corresponding to the CH species found in the plasma which was not present when the spectrum was captured in 100% H_2 environment.

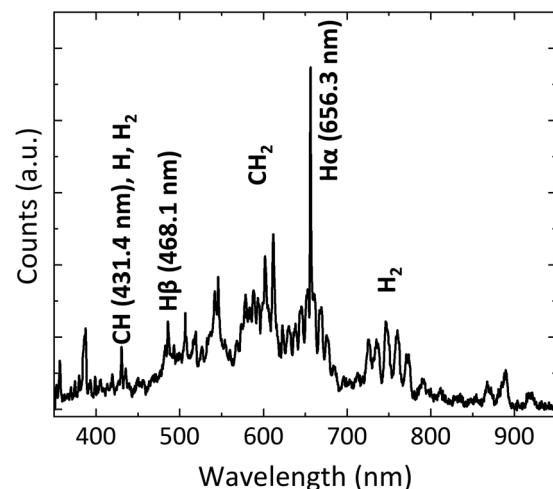


FIG. 2. Captured optical emission spectrum of the plasma formed in a mixture of H_2 with CH_4 environment.

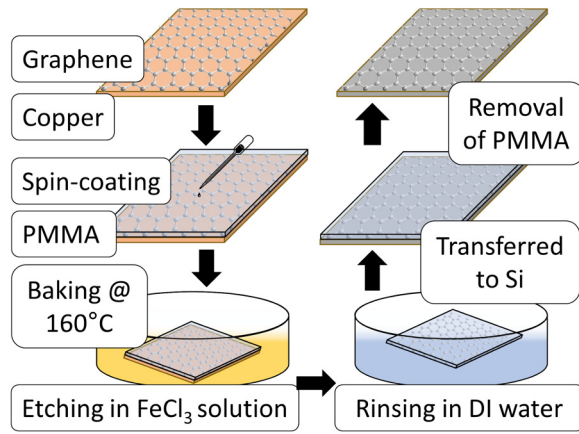


Fig. 3. Graphene transfer process steps using the wet chemical etching method.

C. Graphene transfer process

The deposited graphene is then transferred from the Cu foil substrate onto a silicon (Si) substrate for characterization studies using the wet chemical etching method schematically presented in Fig. 3. A $1.4\ \mu\text{m}$ thick layer of polymethyl methacrylate (MicroChem, 950 PMMA A7) is first spin-coated on top of graphene/copper at 1000 rpm for 45 s and baked at 160°C for 4 min to fully cure. The PMMA layer protects the graphene layer from breaking apart during the later etching steps.^{21,22} The Cu layer, which is approximately $25\ \mu\text{m}$ thick, is then etched from the underside by floating the PMMA/graphene/copper stack on an FeCl_3 solution. After 15–30 min, Cu is completely etched, leaving behind the PMMA/graphene stack. The PMMA/graphene stack is then carefully transferred to a DI water bath to rinse off any residual FeCl_3 solution. This is repeated multiple times and an Si substrate is used to pick up the PMMA/graphene stack. The obtained PMMA/graphene/Si stack is then kept in an oven at 50°C for about 8 h to remove any moisture caught between the graphene and Si interface and to improve the adhesion of graphene on Si. Lastly, an acetone bath is used to remove the PMMA layer leaving behind only the graphene layer on the surface of the Si substrate.

III. RESULTS AND DISCUSSION

A. Raman spectroscopy

After transferring the graphene onto the Si substrate, Raman spectroscopy is used to investigate the quality of the graphene and the respective Raman spectra of the graphene deposited at different temperatures are shown in Fig. 4(a). The presence of the “2D” peak ($2500\text{--}2800\ \text{cm}^{-1}$ band)²³ confirms the ability of remote-plasma CVD method to synthesize graphene at temperatures as low as 600°C . However, the “2D” peak is not observed for the 400°C sample. The presence of “D” peak ($\sim 1350\ \text{cm}^{-1}$ band)²⁴ in the graphene grown using remote plasma-assisted CVD also indicates the presence of disordered carbon in graphene.

Figure 4(b) shows magnified Raman spectra in the range of $1500\text{--}1700\ \text{cm}^{-1}$ with the splitting of “G” into “G”

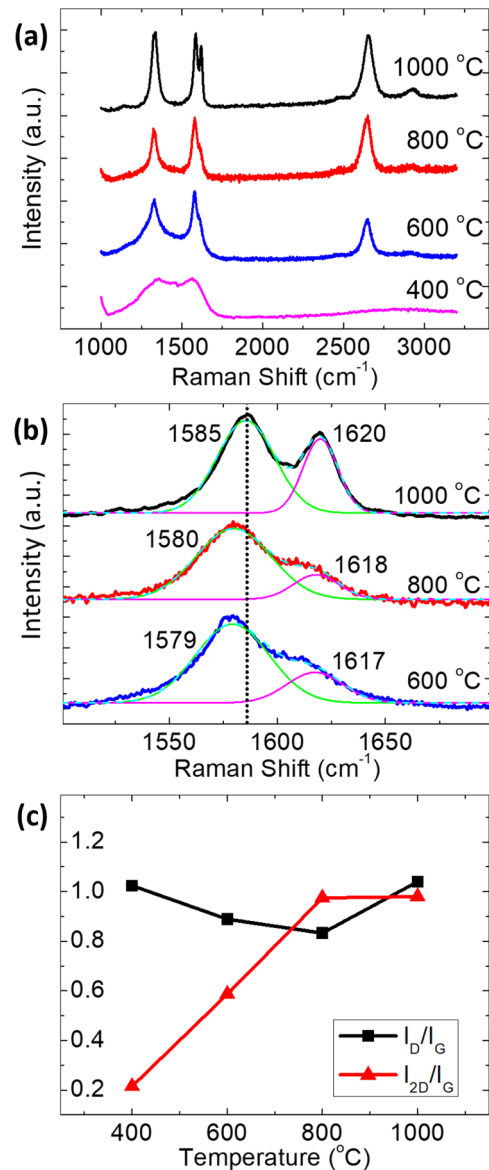


Fig. 4. (a) Raman spectra of the deposited material at various temperatures, (b) magnified view of the “G” and “D” band, and (c) plot of the relative intensity of the “G” band with respect to the “D” and “2D” band.

($\sim 1580\ \text{cm}^{-1}$) and “D” (at a higher wavenumber of about $1620\ \text{cm}^{-1}$) Raman peaks. The presence of “D” peak is attributed to (i) strained graphene²⁵ and (ii) disordered graphene due to the presence of defects and edges.²⁶ The intensity of “D” peak is highest in the sample synthesized at 1000°C and lowest in the sample synthesized at 600°C indicating the least defects in 600°C sample. A shift in the “G” peak position to higher wavenumber value with increasing growth temperature is also indicative of the greater number of graphene layers. The higher temperature, coupled with plasma, causes accelerated reaction rates and excess amounts of activated carbon and these two factors resulted in the formation of multilayer graphene with more defects and disorder.

The I_D/I_G and I_{2D}/I_G ratios for the remote-plasma CVD grown graphene at different temperatures are shown in Fig. 4(c) and can be used to assess the level of disorder in graphene and the number of layers. A smaller I_D/I_G ratio

indicates a lower level of disorder, which suggests that the 800 °C sample has the least disorder. The number of graphene layers can be estimated from I_{2D}/I_G where a value greater than two corresponds to high-quality monolayer graphene while a value lower than two would indicate multilayer graphene formation. Since the I_{2D}/I_G ratio for all the samples is less than two, we can confirm that the graphene deposited using the remote plasma-assisted method is indeed multilayered.

Raman mapping of an area of approximately $35 \times 25 \mu\text{m}^2$ is performed on the 1000 °C graphene sample to confirm that the graphene has been successfully transferred onto the surface of the Si substrate without any visible discontinuities or cracks. Figure 5(a) shows the Raman map of the center region of the Si substrate after the graphene transfer process where the ratio of the characteristic graphene “2D” peak to its baseline value is represented by the scale bar on the left. The signal can be clearly observed throughout the entire region which suggests that most of the graphene has been successfully transferred to the substrate. To further certify the assertion made, Raman mapping was repeated near the graphene edge, refer to Fig. 5(b), where the lower region is the graphene layer while the upper region is uncovered Si. The region without any graphene does not have the characteristic “2D” peak, hence, it is dark in color. This suggests that Raman mapping is a sensitive and useful method to quickly confirm the successful transfer of graphene on a large area.

Using the similar wet chemical etching method as described in Fig. 3, graphene was also successfully transferred to another substrate, polyethylene terephthalate (PET) (Autotex, MacDermid Ltd.). Figure 6 shows the respective

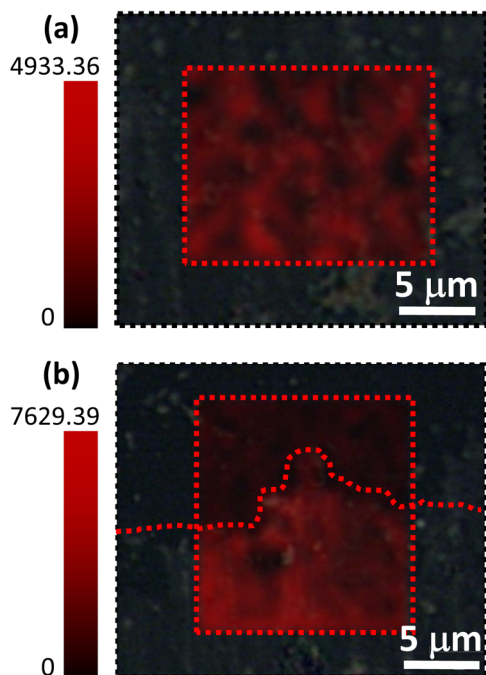


Fig. 5. (a) Raman spectroscopy color mapping of the (a) middle portion of the substrate surface and (b) edge of graphene after the transfer process (color scale corresponds to the ratio of the intensity of the “2D” peak to its baseline value).

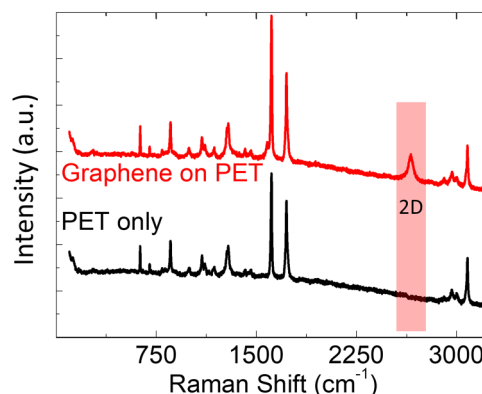


Fig. 6. Raman spectra of the surface of the PET substrate before and after the graphene transfer. The characteristic graphene “2D” peak is indicated by the boxed region.

Raman spectra of the PET surface, before and after the graphene transfer process. This demonstrates the successful transferring of graphene on flexible substrates for the future development of graphene-based flexible wearable devices. Additionally, the good biocompatibility of these materials also makes them suitable for biomedical applications such as biosensors²⁷ or lab-on-a-chip devices.²⁸

To validate the effect of plasma on the graphene growth, conventional thermal CVD without plasma was also used to synthesize graphene. Figure 7 shows the Raman spectrum of the deposited material using thermal CVD without any plasma. At 1000 °C, graphene was grown and transferred successfully on silicon substrates; however, at 800 °C, there is no detectable graphene synthesis for conventional thermal CVD. Therefore, this proves that the successful low-temperature graphene synthesis is indeed due to the effect of the plasma.

B. Scanning electron microscopy

The morphology and size of graphene crystals of the deposited graphene on copper foil observed using scanning electron microscopy (SEM) are shown in Fig. 8. For the 1000 °C sample, there is overcrowding of particles on top of the graphene flakes which could be attributed to the oversourcing of the carbon radical due to both plasma dissociation and large CVD reaction chamber temperature. The 800 °C sample shows uniformly distributed large graphene crystallite flakes ($\sim 100 \times 100 \mu\text{m}^2$), with no overcrowding. At 600 °C, the results are similar to the 800 °C sample. However, for the 400 °C sample, the deposited carbon seems to be very different with the observation of particles and netlike features on the substrate; the large-sized graphene flakes/sheets are not observed to form at this temperature.

In order to investigate the spatial uniformity of the graphene flakes/sheets along the direction of the gas flow, the SEM measurement is repeated at different regions of the Cu foil (see supplementary material³⁰ for the SEM images at different locations). The results showed that the size of the graphene flakes/sheets is consistent for all the sample regions, which suggest that the graphene flakes/sheets are uniform throughout the entire Cu foil. Therefore, there is potential to scale up this method for large area deposition of graphene.

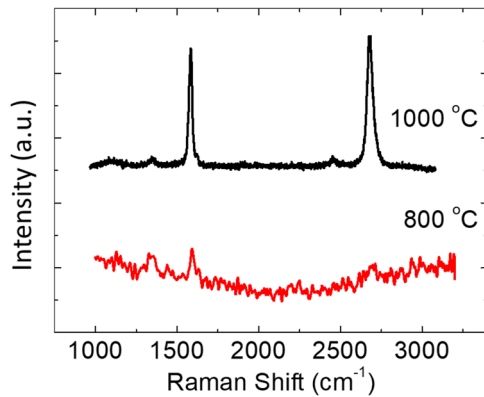


Fig. 7. Raman spectra of the deposited material from thermal CVD at 1000 and 800 °C.

C. Glucose biosensing

A graphene-based electrochemical biosensor was fabricated to demonstrate the potential of using the remote plasma-assisted synthesized graphene for glucose sensing.

First, the graphene was synthesized at 600 °C using the remote-plasma CVD method and transferred onto a PET substrate. Next, two metal contact pads, at a distance of 5 mm apart, were fabricated over the graphene surface. The graphene surface was then cleaned thoroughly by soaking the substrate in a DI water bath for about 8 h. Next, the substrate is placed in a solution containing a concentration of 1 mg/dl of glucose oxidase (GOx, Sigma-Aldrich) for 10 min to allow the immobilization of GOx on the graphene surface. This would be used as a biorecognition molecule for the label-free detection of glucose in a sample fluid. After the graphene surface is functionalized with GOx, a direct current source is applied across the graphene via the metal pads, while the corresponding voltage is measured. The measurement is repeated by adding two different concentrations of β -D-glucose (Cayman Chemical), and the resulting I–V curves are shown in Fig. 9(a).

From the I–V curve, the resistance of the graphene can be obtained by linear curve fitting and the resulting relationship between the glucose concentration and resistance is shown in

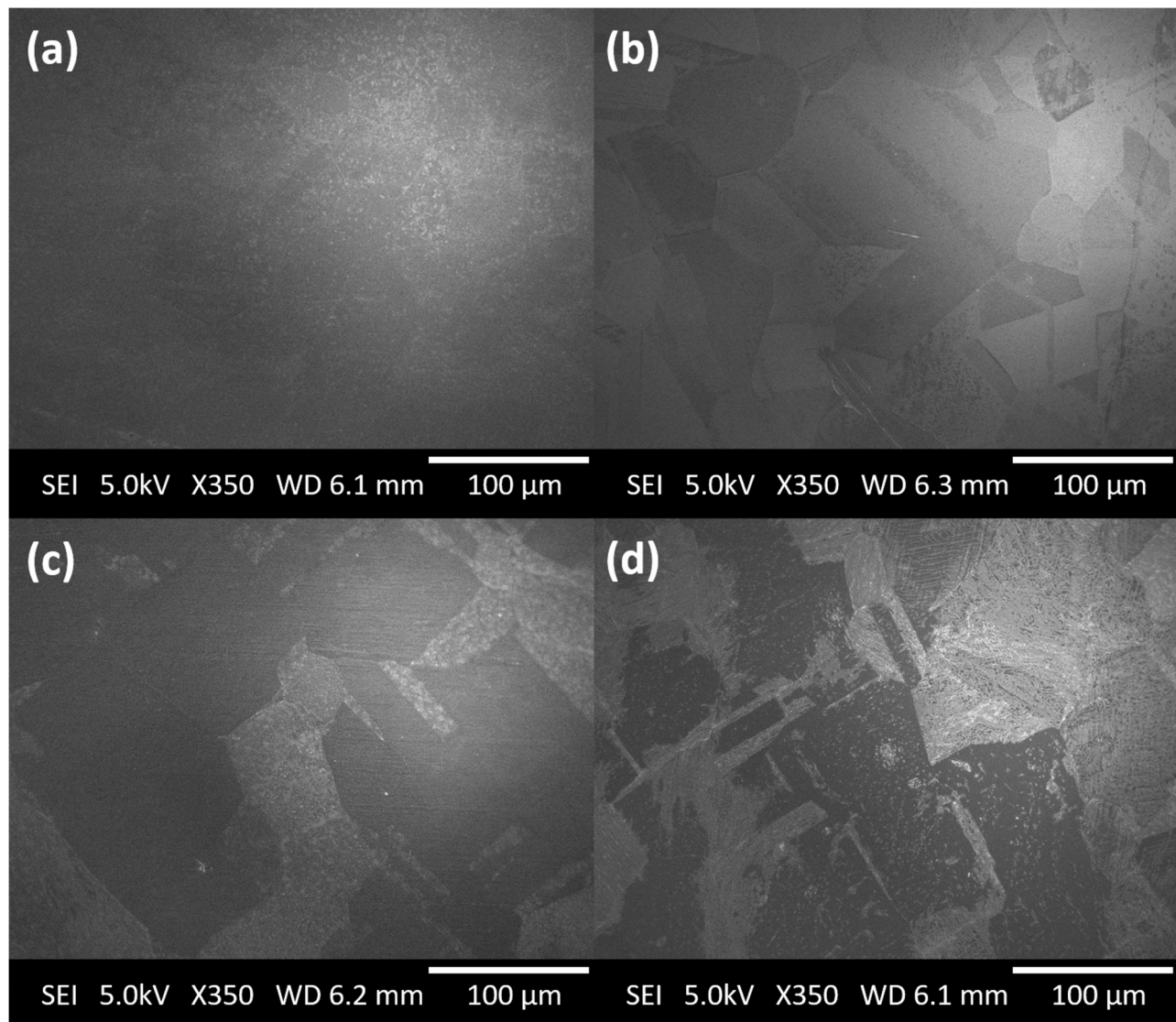


Fig. 8. SEM images of the surface of the copper substrate at (a) 1000 °C, (b) 800 °C, (c) 600 °C, and (d) 400 °C deposition temperatures.

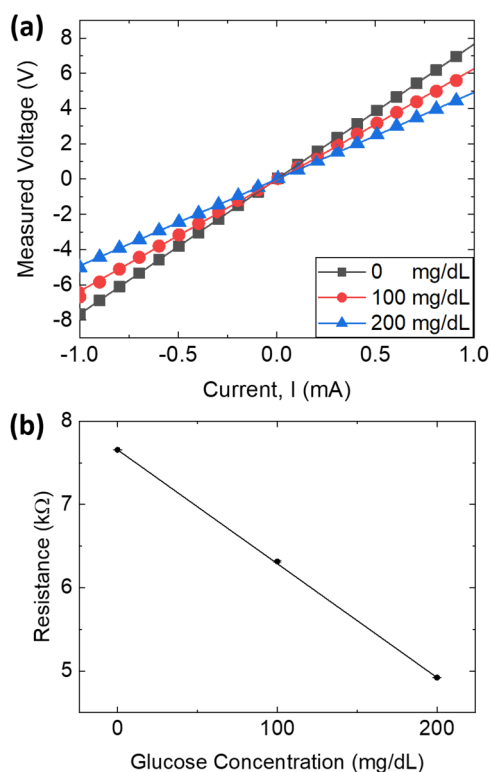


Fig. 9. (a) I-V characteristic curves of the graphene with varying glucose concentration and (b) the change in measured resistance across the graphene.

Fig. 9(b). The resistance when only GOx is present with no glucose is estimated to be 7.66 kΩ. The resistance decreased to 6.31 kΩ in the presence of 100 mg/dl of glucose and further decreased to 4.92 kΩ when the glucose concentration is increased to 200 mg/dl. The reduction of the resistance can be attributed to the improvement to the electron-transfer rate across the surface of the graphene. This is because the GOx would hydrolyze the glucose contained in the sample fluid which produces H⁺ ions.²⁹ The free electrons generated from this process are then transported to the contact pads which is detected as a change in the measured resistance across the biosensor. This allows us to establish the relation between the concentration of the glucose solution and the measured resistance across the graphene which suggests that the developed graphene-based electrochemical biosensor can be useful for label-free glucose sensing.

IV. SUMMARY AND CONCLUSIONS

Low-temperature remote plasma-assisted CVD method has been demonstrated for the growth of large-area horizontal graphene in a short duration of 15 min. SEM and Raman result successfully demonstrate the large area graphene growth with an average crystal size of approximately 100 × 100 μm² even at 600 °C. A graphene-based biosensor has also been fabricated and demonstrated experimentally. It is envisioned that this method could prove to be promising for the direct synthesis of graphene on other substrates with a low melting point. However, further work is necessary to optimize the plasma parameters such as the pressure, power, and concentration of

the carbon precursor feedstock to lower the temperature further for graphene synthesis through remote plasma-assisted technique. Potentially, graphene can be directly deposited on a flexible and stretchable substrate which is useful for the development of wearable electronics of the future.

ACKNOWLEDGMENTS

This research is supported by NIE AcRF Research Grant RI 4/16 RSR provided by the National Institute of Education and MOE Tier 1 Grant RG192/17. J. Y. Pae would also like to acknowledge NTU for the Research Student Scholarship and SC3DP, which is supported by the National Research Foundation, Prime Minister's Office, Singapore under its Medium-Sized Centre funding scheme.

- ¹M. S. A. Bhuyan, M. N. Uddin, M. M. Islam, F. A. Bipasha, and S. S. Hossain, *Int. Nano Lett.* **6**, 65 (2016).
- ²X. Li et al., *Science* **324**, 1312 (2009).
- ³E. O. Polat, O. Balci, N. Kakenov, H. B. Uzlu, C. Kocabas, and R. Dahiya, *Sci. Rep.* **5**, 16744 (2015).
- ⁴A. Walcarus, S. D. Minteer, J. Wang, Y. Lin, and A. Merkoçi, *J. Mater. Chem. B* **1**, 4878 (2013).
- ⁵L. Huang, Q. H. Chang, G. L. Guo, Y. Liu, Y. Q. Xie, T. Wang, B. Ling, and H. F. Yang, *Carbon* **50**, 551 (2012).
- ⁶K. S. Novoselov, A. K. Geim, S. V. Morozov, D. Jiang, Y. Zhang, S. V. Dubonos, I. V. Grigorieva, and A. A. Firsov, *Science* **306**, 666 (2004).
- ⁷H. Tan, D. Wang, and Y. Guo, *Coatings* **8**, 40 (2018).
- ⁸Q. Liu, C. Yu, Z. He, G. Gu, J. Wang, C. Zhou, J. Guo, X. Gao, and Z. Feng, *Appl. Surf. Sci.* **454**, 68 (2018).
- ⁹C. M. Seah, S. P. Chai, and A. R. Mohamed, *Carbon* **70**, 1 (2014).
- ¹⁰C. Y. Chen, D. Dai, G. X. Chen, J. H. Yu, K. Nishimura, C.-T. Lin, N. Jiang, and Z. L. Zhan, *Appl. Surf. Sci.* **346**, 41 (2015).
- ¹¹J. Chan et al., *ACS Nano* **6**, 3224 (2012).
- ¹²H. K. Jeong, J. D. C. Edward, G. H. Yong, and L. Choong Hun, *J. Korean Phys. Soc.* **58**, 53 (2011).
- ¹³A. Malesevic, R. Vitchev, K. Schouteden, A. Volodin, L. Zhang, G. Van Tendeloo, A. Vanhulsel, and C. Van Haesendonck, *Nanotechnology* **19**, 305604 (2008).
- ¹⁴L. Fang, W. Yuan, B. Wang, and Y. Xiong, *Appl. Surf. Sci.* **383**, 28 (2016).
- ¹⁵D. A. Boyd et al., *Nat. Commun.* **6**, 6620 (2015).
- ¹⁶B. Ouyang, Y. Zhang, Z. Zhang, H. J. Fan, and R. S. Rawat, *RSC Adv.* **6**, 23968 (2016).
- ¹⁷Y. Zhang, Z. Li, P. Kim, L. Zhang, and C. Zhou, *ACS Nano* **6**, 126 (2012).
- ¹⁸A. Pastol and Y. Catherine, *J. Phys. D Appl. Phys.* **23**, 799 (1990).
- ¹⁹J. D. Hey, C. C. Chu, and J. P. S. Rash, *J. Quant. Spectrosc. Radiat. Transf.* **62**, 371 (1999).
- ²⁰H. H. Ley, A. Yahaya, and R. K. R. Ibrahim, *Plasma Sources Sci. Technol.* **15**, 42 (2006).
- ²¹G. B. Barin, Y. Song, I. D. F. Gimenez, A. G. S. Filho, L. S. Barreto, and J. Kong, *Carbon* **84**, 82 (2015).
- ²²X. Liang et al., *ACS Nano* **5**, 9144 (2011).
- ²³L. M. Malard, M. A. Pimenta, G. Dresselhaus, and M. S. Dresselhaus, *Phys. Rep.* **473**, 51 (2009).
- ²⁴A. C. Ferrari, *Solid State Commun.* **143**, 47 (2007).
- ²⁵T. M. G. Mohiuddin et al., *Phys. Rev. B Condens. Matter Mater. Phys.* **79**, 205433 (2009).
- ²⁶A. Dey, A. Chroneos, N. S. J. Braithwaite, R. P. Gandhiraman, and S. Krishnamurthy, *Appl. Phys. Rev.* **3**, 021301 (2016).
- ²⁷J. Wu, R. Wang, H. Yu, G. Li, K. Xu, N. C. Tien, R. C. Roberts, and D. Li, *Lab Chip* **15**, 690 (2015).
- ²⁸M. Li, D. Liu, D. Wei, X. Song, D. Wei, and A. T. S. Wee, *Adv. Sci.* **3**, 1600003 (2016).
- ²⁹S. Wu, F. Su, X. Dong, C. Ma, L. Pang, D. Peng, M. Wang, L. He, and Z. Zhang, *Appl. Surf. Sci.* **401**, 262 (2017).
- ³⁰See supplementary material at <https://doi.org/10.1116/1.5093241> for the SEM images at different regions of the growth substrate.